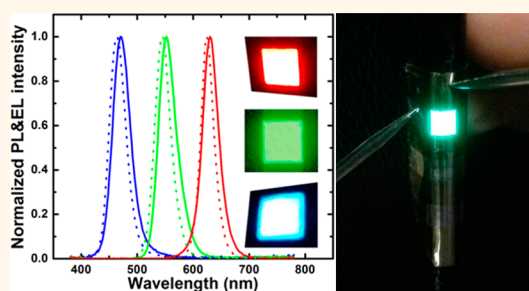


# Highly Flexible, Electrically Driven, Top-Emitting, Quantum Dot Light-Emitting Stickers

Xuyong Yang,<sup>†</sup> Evren Mutlugun,<sup>†,\*||</sup> Cuong Dang,<sup>†</sup> Kapil Dev,<sup>†</sup> Yuan Gao,<sup>†</sup> Swee Tiam Tan,<sup>†</sup> Xiao Wei Sun,<sup>†,\*</sup> and Hilmi Volkan Demir<sup>†,\*,S,\*</sup>

<sup>†</sup>LUMINOUS! Centre of Excellence for Semiconductor Lighting and Displays, School of Electrical and Electronic Engineering, and <sup>‡</sup>School of Physical and Mathematical Sciences, Nanyang Technological University, Nanyang Avenue, Singapore 639798, and <sup>§</sup>Department of Electrical and Electronics Engineering and Department of Physics, UNAM—Institute of Materials Science and Nanotechnology, Bilkent University, Bilkent, Ankara, Turkey 06800. <sup>||</sup>Present address: Department of Electrical-Electronics Engineering, Abdullah Gul University, Kayseri, Turkey 38039.

**ABSTRACT** Flexible information displays are key elements in future optoelectronic devices. Quantum dot light-emitting diodes (QLEDs) with advantages in color quality, stability, and cost-effectiveness are emerging as a candidate for single-material, full color light sources. Despite the recent advances in QLED technology, making high-performance flexible QLEDs still remains a big challenge due to limited choices of proper materials and device architectures as well as poor mechanical stability. Here, we show highly efficient, large-area QLED tapes emitting in red, green, and blue (RGB) colors with top-emitting design and polyimide tapes as flexible substrates. The brightness and quantum efficiency are 20 000 cd/m<sup>2</sup> and 4.03%, respectively, the highest values reported for flexible QLEDs. Besides the excellent electroluminescence performance, these QLED films are highly flexible and mechanically robust to use as electrically driven light-emitting stickers by placing on or removing from any curved surface, facilitating versatile LED applications. Our QLED tapes present a step toward practical quantum dot based platforms for high-performance flexible displays and solid-state lighting.



**KEYWORDS:** quantum dot · polyimide tape · flexibility · electroluminescence · light-emitting diodes

Colloidal quantum dot light-emitting diodes (QLEDs) have recently received considerable attention for next-generation lighting and display systems due to their narrow emission line width,<sup>1–4</sup> high brightness,<sup>5,6</sup> color tunability,<sup>7,8</sup> and cost-effective fabrication techniques.<sup>9–13</sup> The strong quantum confinement effect in semiconductor nanocrystals allows one to engineer their emission color across the full visible spectrum just by changing their size in simple colloidal synthesis methods, realizing full color, single-material LEDs. Rapid progress has been made in QLEDs' performance during their two decades of development.<sup>14</sup> Now, QLEDs are emerging as an undeniable competitor to organic light-emitting diodes (OLEDs) for lighting and display applications.<sup>15,16</sup> QLEDs, typically using a QD film thickness of less than 100 nanometers, are very thin, making them virtually transparent and flexible, the key elements that OLEDs have successfully demonstrated for future

information displays.<sup>17,18</sup> However, challenges remain in the development of flexible QLEDs due to the specific requirements of electrodes and flexible substrates for device fabrication and operation. Indium tin oxide (ITO) is still the main electrode material for flexible and nonflexible QLEDs,<sup>19,20</sup> but its brittle nature<sup>17</sup> is not quite suitable for flexible optoelectronic devices. QLED fabrication involves multiple steps of solution-processed techniques with various chemicals and high-temperature annealing, therefore limiting the device architecture designs and the choices of suitable flexible plastic substrates. For example, aqueous polyethylene dioxythiophene:polystyrene-sulfonate (PEDOT:PSS), which is widely used as a buffer layer for QLED fabrication, is generally annealed at ~150 °C, to remove solvents and functionalize this charge injection layer.<sup>21,22</sup> Such high-temperature annealing usually causes the destruction or distortion of flexible substrates. In addition,

\* Address correspondence to volkan@stanfordalumni.org (H. V. Demir); exwsun@ntu.edu.sg (X. W. Sun).

Received for review May 12, 2014 and accepted July 14, 2014.

Published online July 14, 2014  
10.1021/nn502588k

© 2014 American Chemical Society

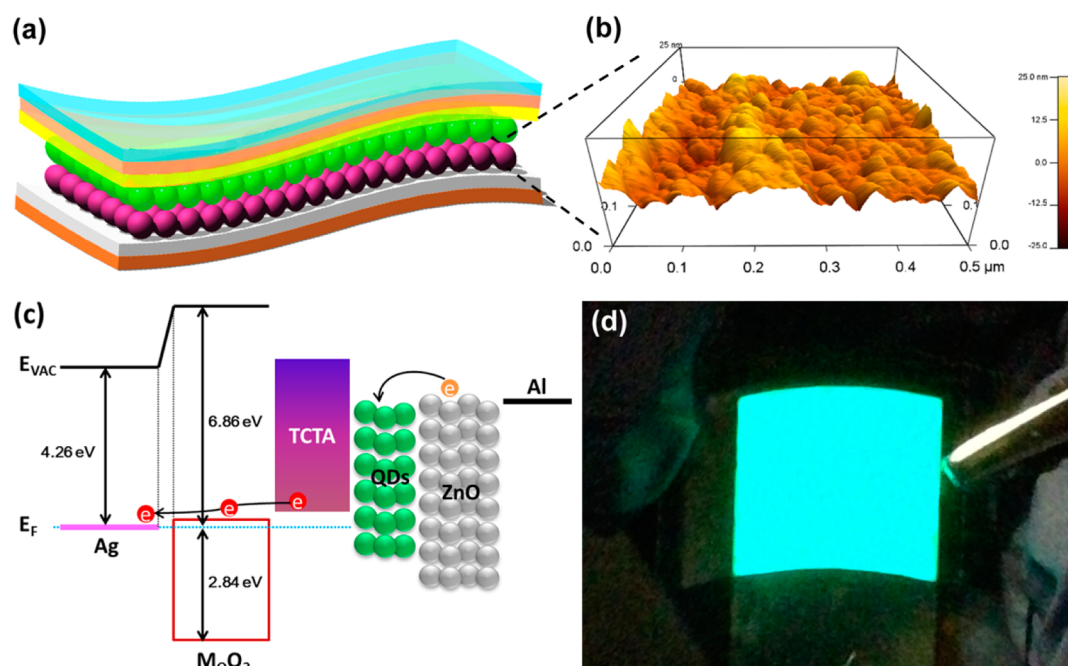


**Figure 1.** (a) Schematic of the QLED film configuration (from the bottom to the top): Kapton tape/Al/ZnO NPs/QDs/TCTA/MoO<sub>3</sub>/Ag. The CdSe/ZnS QD and ZnO NP layers were deposited by the spin-casting method, and other layers were deposited by thermal evaporation. (b) AFM image of spin-coated ZnO nanoparticle ETL formed on the Kapton tape/Al surface. (c) Energy level diagram of the QLED film. (d) Photographic image of a large-area QLED tape placed on a flexible plastic substrate (20 mm × 25 mm).

only a few types of plastic such as poly(ethylene-terephthalate) (PET) can be used as flexible substrates because common solvents, e.g., toluene, often damage organic substrates. Relaxing these requirements to achieve flexible QLEDs results in greatly limited device performance.

Here, we report flexible top-emitting QLED tapes employing inverted device architecture with Kapton polyimide as the substrate and metallic thin films (Al, Ag) as the electrodes. Highly flexible Kapton polyimide films are stable against many organic solvents and can withstand relatively high temperatures (~260 °C), which allowed us to optimize them for the best device performance. Such highly flexible top-emitting QLED films demonstrate maximum brightness and efficiency values of 20 000 cd m<sup>-2</sup> and 4.03%, which are the highest performance values for flexible QLEDs reported to date. By controlling the quantum dot (QD) emission wavelength during colloidal synthesis, we achieved flexible QLED tapes with very high performance in all three colors: red, green, and blue (RGB). As an additional advantage of the Kapton tape (optionally one side with adhesive) and the mechanically robust structure, our QLED films can be easily placed on (and removed from) essentially any three-dimensional surface, even with a very large active area of 2 cm × 2.5 cm, the largest flexible QLED. The uses are akin to QLED stickers. These results demonstrate a practical route toward flexible QLEDs for information display applications.

## RESULTS AND DISCUSSION

The top-emitting device architecture was demonstrated in inorganic and organic LEDs with advantages

of enhanced aperture ratio of display.<sup>23</sup> We first employed this architecture to design our flexible QLED films, as top-emitting LEDs are of increasing interest since the light outcoupling from the top allows LED devices on opaque substrates, which is quite useful for many applications such as high-resolution active matrix (AM) displays.<sup>24,25</sup> The corresponding structure of our QLED films comprises a multilayer thin film architecture of Kapton tape/Al/ZnO nanoparticles (NPs)/QDs/2,2',2''-tris(*N*-carbazoly)triphenylamine (TCTA)/MoO<sub>3</sub>/Ag, as shown in Figure 1a. The thickness of the Ag layer (anode) on top of the device was optimized at 18 nm to balance between conductivity and transmissibility for the best device performance. The CdSe/ZnS core-shell-structured QDs, prepared by a one-pot synthesis method,<sup>3</sup> were used as the emissive layer. The ZnO nanoparticle film serving as the electron transport layer (ETL) was spin-casted from ZnO nanoparticles in butanol solution. Note that, although the high-quality ZnO nanoparticle films deposited on ITO have been achieved before, the present case is quite different with the ZnO nanoparticle film on Al. Because of the obvious distinction in their surface properties such as surface energy and hydrophobic/hydrophilic nature,<sup>26</sup> ZnO nanoparticle films form multiple small cracks and some large broken areas on Al (Supporting Information Figure S1). In our work, we achieved uniform ZnO nanoparticle films by the modification of the surface properties of ZnO NPs. The ZnO NPs employed here were prepared with an approach modified from that previously reported by a solution-precipitation process.<sup>9</sup> The surface ligands of the ZnO NPs were removed

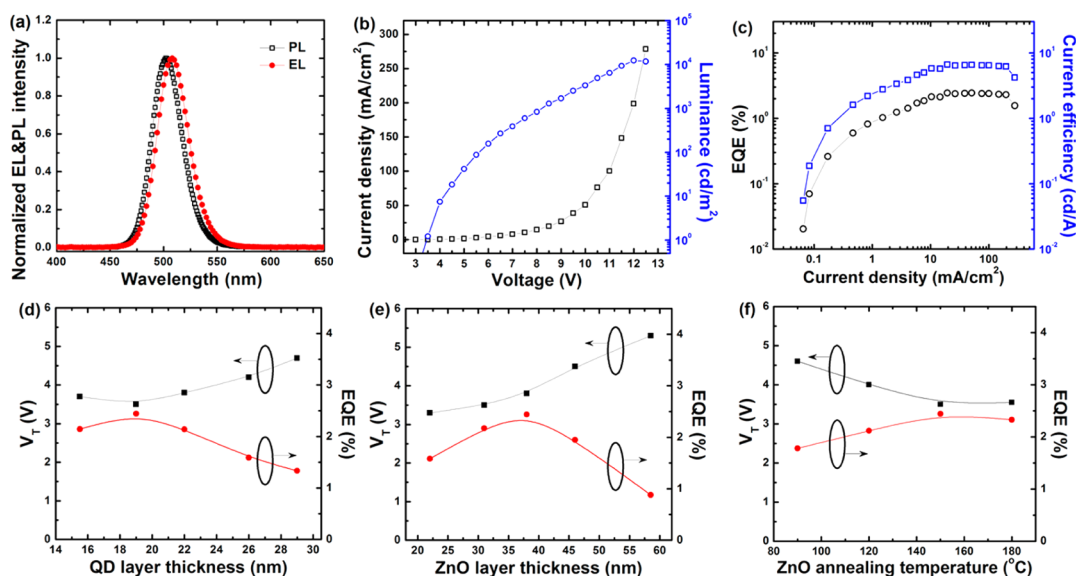


**Figure 2.** (a) Normalized PL and EL spectra of QDs and a typical QLED tape at an applied voltage of 6 V. (b) Current density and peak luminance of the QLED films as a function of bias voltage. (c) External quantum efficiency (EQE) and current efficiency (CE) of the QLED tapes as a function of current density. (d) Turn-on voltage ( $V_T$ ) and maximum EQE vs QD layer thickness (ZnO nanoparticle layer thickness of 38 nm). The turn-on voltage is defined as the voltage at which the luminance is  $1 \text{ cd m}^{-2}$ . (e)  $V_T$  and maximum EQE vs ZnO nanoparticle layer thickness (QD layer thickness of 19 nm). (f)  $V_T$  and maximum EQE vs ZnO nanoparticle layer annealing temperature (thickness of QD and ZnO nanoparticle layers is 19 and 38 nm, respectively).

by adding excess precipitant solvent (hexane/ethanol), and then the resulting white precipitant was dispersed into butanol. As shown in Figure 1b, the surface roughness (RMS) of the film made from a ZnO nanoparticle butanol solution is only 3.6 nm, about the size of ZnO nanoparticles and the RMS of Kapton tape (Supporting Information Figure S2), indicating excellent surface smoothness. The schematic energy level diagram of the device depicted in Figure 1c shows that the electrons can easily be injected from the Al to the QD layer via the conduction band of the ZnO nanoparticle layer. However, the case is different for the hole injection.<sup>27–29</sup> For n-doped  $\text{MoO}_3$ , owing to the deep lying electronic states of  $\text{MoO}_3$ , the hole injection from anode to the organic semiconductor (TCTA) results from carrier breakthrough from the  $\text{MoO}_3/\text{TCTA}$  junction. The electrons are extracted from the highest occupied molecular orbital (HOMO) level of TCTA through the conduction band of  $\text{MoO}_3$ . Figure 1d displays bright, uniform, and saturated green QD emission from our flexible QLED film with a surface area of  $2 \text{ cm} \times 2.5 \text{ cm}$ , which is the largest area reported for flexible QLEDs so far. The uniform size of QDs and ZnO nanoparticles and no bubbles in the Kapton tape substrate in the device fabrication process are required for obtaining such large-area flexible devices.

Figure 2a presents the electroluminescence (EL) spectrum of our typical green QLED tapes. The pure QD emission at a peak wavelength of  $\sim 508 \text{ nm}$  with a full width at half-maximum (fwhm) of 34 nm illustrates the highly efficient recombination of electrons and holes in the QD emissive layer. The peak wavelength is red-shifted ( $\sim 6 \text{ nm}$ ) from the QD solution's

photoluminescence (PL) resulting from a combination of finite dot-to-dot interactions in close-packed solid films and the electric-field-induced Stark effect. The typical current density and luminance curves as a function of applied voltage for the unpackaged QLED films are shown in Figure 2b. The maximum luminance reaches  $12\,300 \text{ cd/m}^2$ , and the turn-on voltage ( $V_T$ ) of 3.5 V is relatively low, suggesting a small barrier height for the charge injection into the QDs. In addition, the external quantum efficiency–current efficiency–current density (EQE–CE–J) characteristics of the QLED film exhibit high device efficiency, with a maximum EQE of 2.44% and CE of 6.61 cd/A (Figure 2c). The ZnO nanoparticles as ETLs in the inverted QLEDs help to neutralize QDs, *i.e.*, turning dark (charged) QDs to bright (neutral) QDs, and, therefore, improve the device performance.<sup>1</sup> But like other metal oxides, ZnO also quenches the quantum yield of QDs due to an ultrafast nonradiative process that depends on the proximity of emitters to the interface. The two opposite effects imply that the device performance is strongly dependent on the thickness of the QD and ZnO nanoparticle layers.<sup>9</sup> Figure 2d and e show the turn-on voltage  $V_T$  and maximum EQE as a function of the QD and ZnO nanoparticle layer thickness for the QLED tapes. With the ZnO layer fixed at  $\sim 38 \text{ nm}$ , the lowest  $V_T$  of 3.5 V and the maximum EQE of 2.44% can be achieved when the device has a 19 nm thick QD layer (Figure 2d), which is equivalent to three QD monolayers. This result is consistent with the previous reports that a few monolayers of QDs are needed for efficient recombination of electrons and holes to provide exciton formation in the QDs.<sup>15</sup> For a 19 nm thick QD layer,

increasing the ZnO layer thickness from 20 nm to 60 nm resulted in a continuous increase of  $V_T$  from 3.3 V to 5.3 V, while the highest EQE value is achieved when the ZnO thickness is 38 nm (Figure 2e). This implies that a finite voltage is needed across the ZnO layer, making the efficiency of the device with a thicker ZnO nanoparticle layer dramatically decrease. In addition to the above factors, we found that the annealing treatment of the ZnO nanoparticle film to reduce the defects can also improve the device performance significantly. As shown in Figure 2f, for a QLED tape with a 19 nm thick QD layer and a 38 nm thick ZnO nanoparticle layer, increasing the ZnO annealing temperature from 90 °C to 180 °C, decreases the  $V_T$  steadily until 150 °C and the EQE increases to the maximum level of 2.44% at 150 °C. After that, the EQE and  $V_T$  are almost unchanged with increasing annealing temperature. We believe that this is enabled by enhancing the electron transport in ZnO nanoparticle films, which is associated with the reduction in defect concentration of ZnO nanoparticles.

To further confirm the effect of defects in ZnO nanoparticles in the device's EL performance, we compared the PL intensity of ZnO nanoparticle films annealed at different temperatures with an excitation source of 300 nm wavelength. As shown in Figure 3, the PL spectra of ZnO nanoparticles consist of a sharp UV emission

band and a broad green emission band peaking at 550 nm. The narrow UV emission is attributed to the radiative annihilation of excitons,<sup>30</sup> while the broad visible emission is associated with defects in ZnO nanoparticles.<sup>31</sup> The origin of defect emission has been the subject of ongoing debate, and the widely accepted theory is that they are caused by the oxygen vacancies or zinc interstitials.<sup>32,33</sup> In addition, it can be noted that the PL intensities of the broad green emission band dramatically decrease with the annealing temperature increasing from 90 °C to 150 °C. Beyond 150 °C, there is no obvious green emission observed from ZnO. In contrast, the UV emission intensities vary only slightly, suggesting that the total defect concentration in ZnO is significantly decreased with increasing annealing temperature. Combined with the observed EQE and  $V_T$  trends in the case of QLED films, these results show a good correlation between the device EL performance and defect concentration in ZnO nanoparticles. The significant reduction in the defect concentration and increase in the crystal quality of ZnO nanoparticles improve the electron transport due to the decrease in defect-trapped electrons in ZnO (Supporting Information Figure S3), resulting in enhanced EL intensity. It should be noted that the annealing temperature of 150 °C is too high for most flexible substrates, which may limit the QLED device performance to a great extent, while this is fine for Kapton polyimide films.

The thin Ag layer (~18 nm) serves as a semitransparent anode in our top-emitting QLED tapes, and an organic capping (OC) layer on top of the Ag layer could modify the device's optical structure as the change of interference effects within the device.<sup>34</sup> The OC layer has been demonstrated to improve the outcoupling efficiency of the top-emitting OLED.<sup>35</sup> Here, we deposited a tris-8-hydroxyquinoline aluminum ( $Alq_3$ ) film as a capping layer above the top contact. Figure 4 shows the performance of the device with the OC layer as measured in the vertical direction. We improved the device performance significantly just by adding the optical outcoupling  $Alq_3$

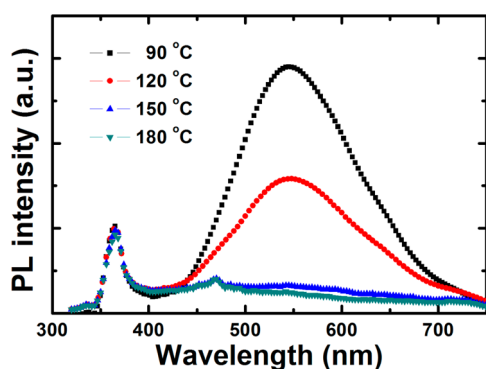


Figure 3. Room-temperature PL spectra for ZnO nanoparticle films annealed at different temperatures from 90 to 180 °C.

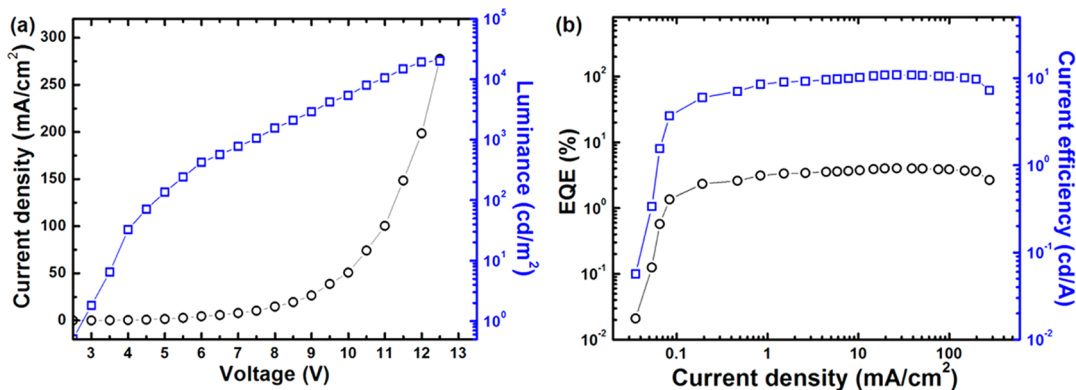


Figure 4. (a) Current density and luminance of QLED tape as a function of applied voltage. (b) External quantum efficiency and current efficiency of QLED tape as a function of current density.

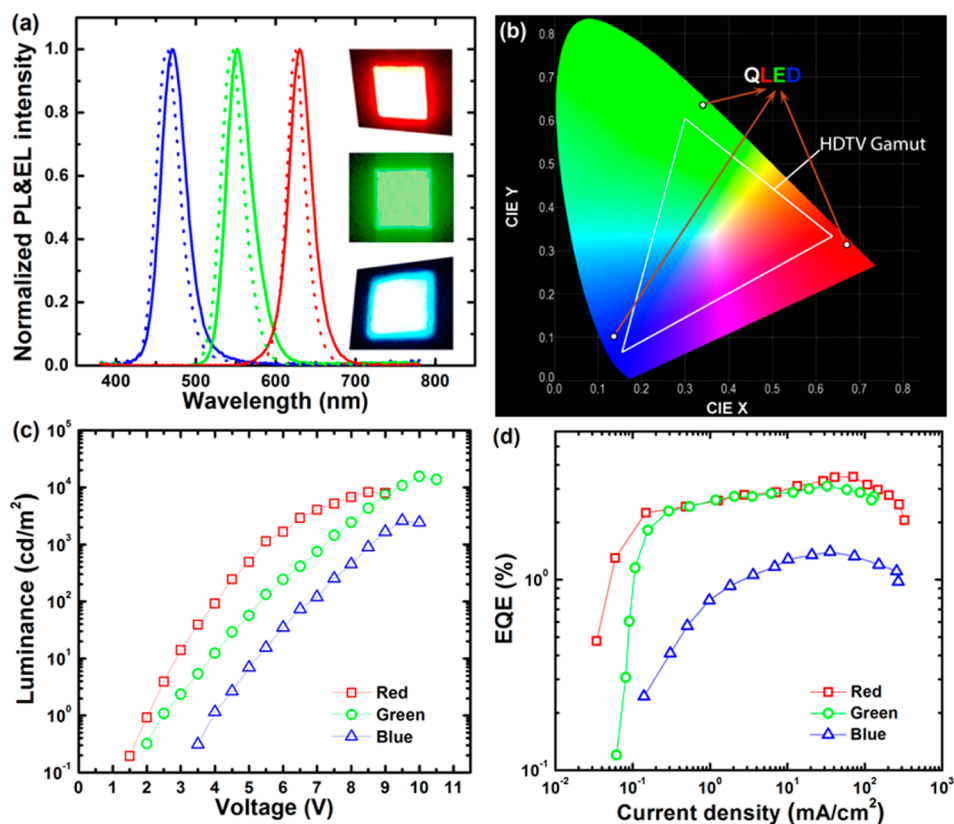


Figure 5. (a) Normalized EL spectra of QLED films with peak emission wavelengths of 470 nm (blue), 551 nm (yellowish green), and 630 nm (red). Inset: Photographic images of the RGB QLED tapes. (b) CIE coordinates of the three devices together with the HDTV color standards. (c) Luminance of our RGB QLED films as a function of applied voltage. (d) External quantum efficiency of QLED tapes as a function of current density.

layer with a film thickness of 40 nm. The maximum brightness reaches 20 000  $\text{cd}/\text{m}^2$  (Figure 4a), and an EQE level of 4.03% and a current efficiency value of 10.9  $\text{cd}/\text{A}$  can be achieved at a current density of 26.6  $\text{mA}/\text{cm}^2$  (Figure 4b). The thin OC layer improves the efficiency and the brightness of our flexible QLED film by 165% and 162%, respectively.

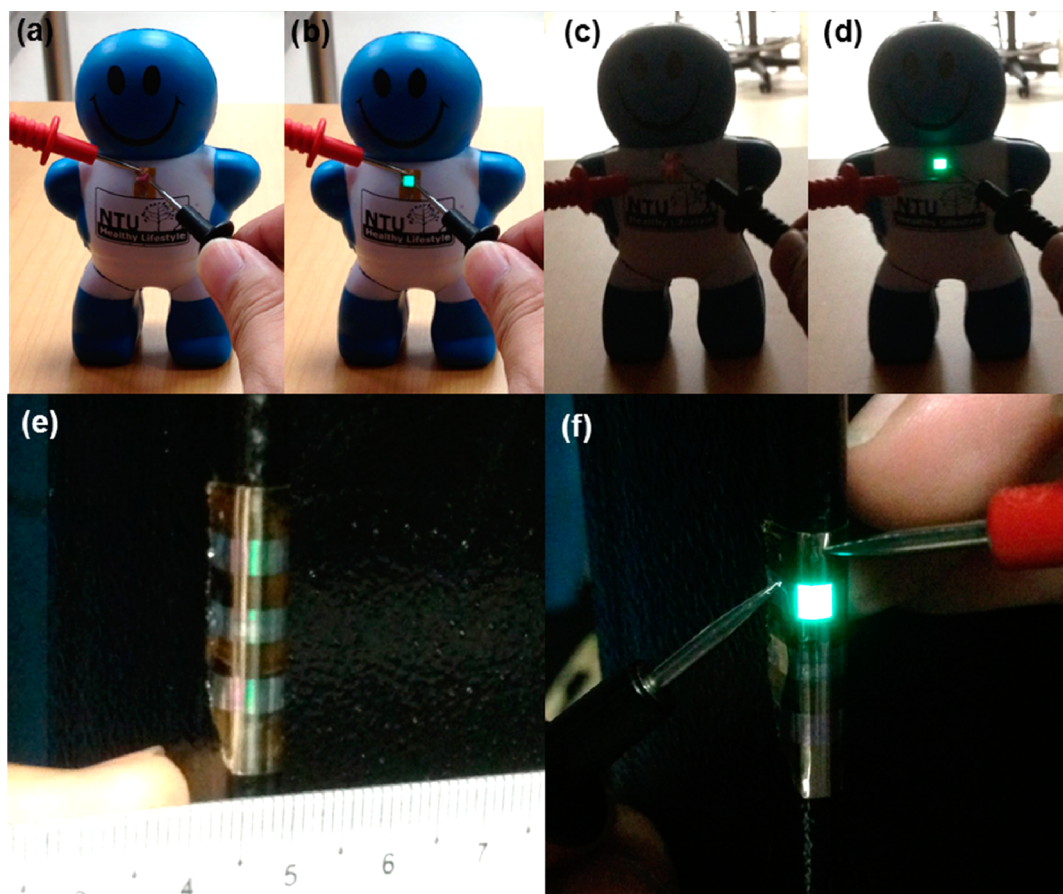
Using our optimized structure with multicolored quantum dots, we obtained RGB-emitting QLED tapes. Figure 5a presents the normalized EL spectra of these QLED films with three different peak emission wavelengths (470, 551, and 630 nm) at the applied voltage of 6 V. It can be observed that all the EL spectra are saturated with QD emission and are slightly red-shifted (5–6 nm) from the corresponding PL spectra of QD solutions. The fwhm is 33, 37, and 37 nm for the respective RGB colors. The inset shows photographic images of the three operating devices, which display nearly saturated color emission. As shown by the Commission Internationale de Eclairage (CIE) chromaticity diagram in Figure 5b, these QLED films cover a larger area than a high-definition television (HDTV) standard color triangle.<sup>15</sup> The luminance and EQE as a function of the current density for the optimized QLED films are shown in Figure 5c and d. The maximum luminance and EQE values of 2600  $\text{cd m}^{-2}$  and 1.40% for the blue emission (peak at 470 nm), 15 600  $\text{cd m}^{-2}$

TABLE 1. Summary of the Optical and Electrical Properties of QDs and QLED Tapes

	PL $\lambda_{\text{max}}$	EL $\lambda_{\text{max}}$	fwhm	$V_{\text{T}}$	EQE <sub>max</sub>		CIE index
color of QLED	(nm)	(nm)	(nm)	(V)	(%)	$L_{\text{max}}$ ( $\text{cd}/\text{m}^2$ )	(x, y)
blue	465	470	37	3.9	1.40	2600	0.135, 0.103
green	502	508	34	3	4.03	20 000	0.086, 0.643
yellowish-green	545	551	37	2.5	3.09	15 600	0.335, 0.631
red	624	630	33	2	3.46	8200	0.682, 0.315

and 3.09% for the yellowish green emission (at 551 nm), and 8200  $\text{cd m}^{-2}$  and 3.46% for the red emission (at 630 nm) were achieved. Table 1 summarizes the detailed performance parameters of our RGB QLED tapes. The maximum luminance and efficiency are the highest values reported to date for correspondingly colored flexible QLEDs. Nevertheless, it still can be expected that further optimization such as improving the quantum yields of QD films would realize better device performances.

In addition to the optoelectrical high performance, the distinct advantages of our top-emitting QLED tapes over previous flexible QLEDs are their highly flexible and mechanically robust structure. With the use of Kapton tape, our QLED stickers are easily placed on or removed from almost any three-dimensional surface, which facilitates the versatile use of our QLED platform.



**Figure 6.** Photographic images of a QLED tape with a pixel size of  $3\text{ mm} \times 3\text{ mm}$  placed on different nonplanar surfaces. (a, b) "Off" and "On" device placed on a mascot in a bright room, respectively. (c, d) "Off" and "On" device placed on the mascot in a dark room, respectively. (e, f) "Off" and "On" device placed on a thin steel plate under room light, respectively.

As shown in Figure 6a–d, the green-emitting QLED tape, stuck on a mascot, works very well with high brightness under room light or dark conditions. Furthermore, the operating QLED film can be bent arbitrarily and is free of cracks and dark spots even under almost completely folded bending. As shown in Figure 6e,f, the working QLED tape is placed and bent around a very thin steel plate. Its brightness and uniformity do not show any degradation. The excellent mechanical robustness of our QLED tapes allows us to use them as light-emitting stickers, *i.e.*, a luminescent sticker for three-dimensional surfaces. Its robustness is further confirmed by the device bending test (Supporting Information Figure S4), The brightness remains at 90% after being bent 300 times on a 4 mm diameter rod, whereas with bending on a 12 mm diameter rod there is almost no obvious change in the brightness even after repeating 500 times.

## CONCLUSION

In conclusion, we have demonstrated highly flexible, large-area, full-color, top-emitting QLED tapes with record high efficiency in flexible QLEDs. These superior performances were achieved by the efficient design of a top-emitting device architecture with the proper choice of Kapton tape as the flexible substrate, the surface modification of ZnO nanoparticles for an efficient electron-transporting layer, and the deposition of an Alq<sub>3</sub> capping layer as an outcoupling element. These large-area, ITO-free QLED films also show excellent mechanical robustness and can be used as electrically driven light-emitting stickers on any three-dimensional surface, which enables the extensive and versatile use of LEDs. Our results illustrate a further step toward the practical application of flexible QLEDs in optoelectronic devices including flexible, full-color information displays and surface lighting.

## METHODS

**Materials.** Cadmium oxide (CdO; 99.99+%, Aldrich), zinc acetate (Zn(AcEt)<sub>2</sub>; 99.99%, Aldrich), oleic acid (OA; 90%, Aldrich), 1-octadecene (1-ODE; 90%, Aldrich), tri-*n*-octylphosphine

(TOP, 90%, Aldrich), selenium (Se; 99.99%, Aldrich), sulfur (S; 99.5+%, Sigma-Aldrich), fluorescein-27 (90+%, Sigma), dimethyl sulfoxide (DMSO; 99.98%, Fisher Scientific UK Limited), tetramethylammonium hydroxide pentahydrate (97%, Sigma),

methanol (AR), ethanol (AR), butanol (AR), hexane (AR), acetone (AR), and toluene (AR) were used as received without further purification. The TCTA, Alq<sub>3</sub>, and MoO<sub>3</sub> used for device fabrication were purchased from Luminescence Technology Corp. Kapton tape substrate was purchased from Dakin Engineering Pte Ltd.

**Synthesis of Multicolored QDs and ZnO Nanoparticles.** Green- and blue-emitting CdSe/ZnS QDs with chemical composition gradients were prepared using a one-pot synthesis method,<sup>3</sup> and the red-emitting CdSe/CdS/ZnS core-shell-structured QDs were prepared by the multiple injection method according to the same literature. For a typical preparation of green-emitting QDs, 0.1 mmol of cadmium oxide, 4 mmol of zinc acetate, and 5 mL of oleic acid were loaded in a 50 mL three-neck flask and heated to 150 °C under vacuum to form cadmium oleate (Cd(OA)<sub>2</sub>) and zinc oleate (Zn(OA)<sub>2</sub>). Then 20 mL of 1-octadecene was added to the reaction flask, and the reactor was then filled with nitrogen and heated to 300 °C. At the elevated temperature, 1.6 mL of tri-*n*-octylphosphine with 0.15 mmol of selenium and 4 mmol of sulfur was injected into the flask swiftly, and the reaction mixture was maintained at 300 °C for 10 min for the QD growth. To purify the synthesized QDs, the reaction mixture was cooled to room temperature, and the QDs were extracted by the addition of acetone and methanol, followed by centrifugation. The as-prepared QDs were readily dispersed in toluene. The purified QDs with an average particle size of ~7 nm were measured to give a quantum yield of ~60% in toluene by comparing the fluorescence intensities with a standard reference dye, fluorescein-27.

ZnO nanoparticles with a typical mean diameter of 3–4 nm were synthesized based on a solution-precipitation process.<sup>9</sup> For a typical synthesis, zinc acetate in DMSO (0.1 M, 20 mL) and tetramethylammonium hydroxide in ethanol (0.55 M, 20 mL) were mixed and stirred for 1 h in ambient air, then washed at least four times with excess precipitant solvents such as hexane/ethanol (1:4 by volume), and then the as-prepared white precipitant was dispersed in butanol at a concentration of ~25 mg mL<sup>-1</sup>.

**Fabrication of QLED Devices.** The Kapton tape was wiped by cotton tips with DI-water and acetone first, and the Al cathode (190 nm) was then deposited on top. The ZnO nanoparticle layer was then spin-coated on the Al cathode deposited Kapton tape from a ZnO butanol solution at 500–6000 rpm for 60 s and annealed at 150 °C for 30 min in a nitrogen glovebox. Next, the QD layer was deposited on the ZnO NPs layer by spin-coating the QD dispersion (QDs were dispersed in toluene at 15 mg/mL) at a rate of 1000–6000 rpm for 60 s and cured at 90 °C for 30 min. After that, the TCTA (60 nm), MoO<sub>3</sub> (10 nm), and Ag (18 nm) layers were thermally deposited under a base pressure of ~2 × 10<sup>-4</sup> Pa.

**Instrumentation.** The EL spectra of the flexible QLED films were measured using a Photo Research PR705 Spectra Scan spectrometer, while the luminance–current–voltage characteristics of the devices were measured simultaneously with a programmable Yokogawa GS610 source meter and a Konica Minolta LS-110 luminance meter in air at room temperature. Atomic force microscopy (Cypher AFM, Asylum Research) was used to characterize the morphology of the ZnO nanoparticle films. The PL spectra were recorded using a Shimadzu RF-5301PC spectrofluorophotometer equipped with a 150 W xenon lamp as the excitation source. A four-point probe instrument (CMT-SR2000N) was employed to measure the conductivity of the ZnO nanoparticle films. All measurements were carried out at room temperature under ambient conditions.

**Conflict of Interest:** The authors declare no competing financial interest.

**Acknowledgment.** The authors would like to acknowledge the financial support from Singapore National Research Foundation under NRF-RF-2009-09, NRF-CRP-6-2010-02, NRF-CRP-11-2012-01, and NRF-CRP-11-2012-01 and the Science and Engineering Research Council, Agency for Science, Technology and Research (A\*STAR) of Singapore (project nos. 092 101 0057 and 112 120 2009).

**Supporting Information Available:** Digital optical microscopic images of ZnO nanoparticle films deposited on Al electrodes, AFM image of Kapton tape surface, electrical conductivities of ZnO nanoparticle films, and bending test of QLED films. This material is available free of charge via the Internet at <http://pubs.acs.org>.

## REFERENCES AND NOTES

- Mashford, B. S.; Stevenson, M.; Popovic, Z.; Hamilton, C.; Zhou, Z.; Breen, C.; Steckel, J.; Bulovic, V.; Bawendi, M.; Coe-Sullivan, S.; *et al.* High-Efficiency Quantum-Dot Light-Emitting Devices with Enhanced Charge Injection. *Nat. Photonics* **2013**, *7*, 407–412.
- Cho, K. S.; Lee, E. K.; Joo, W. J.; Jang, E.; Kim, T. H.; Lee, S. J.; Kwon, S. J.; Han, J. Y.; Kim, B. K.; Choi, B. L.; *et al.* High-Performance Crosslinked Colloidal Quantum-Dot Light-Emitting Diodes. *Nat. Photonics* **2009**, *3*, 341–345.
- Bae, W. K.; Kwak, J.; Lim, J.; Lee, D.; Nam, M. K.; Char, K.; Lee, C.; Lee, S. Multicolored Light-Emitting Diodes Based on All-Quantum-Dot Multilayer Films Using Layer-by-Layer Assembly Method. *Nano Lett.* **2010**, *10*, 2368–2373.
- Lee, K.-H.; Lee, J.-H.; Song, W.-S.; Ko, H.; Lee, C.; Lee, J.-H.; Yang, H. Highly Efficient, Color-Pure, Color-Stable Blue Quantum Dot Light-Emitting Devices. *ACS Nano* **2013**, *7*, 7295–7302.
- Kwak, J.; Bae, W. K.; Lee, D.; Park, I.; Lim, J.; Park, M.; Cho, H.; Woo, H.; Yoon, D. Y.; Char, K.; *et al.* Bright and Efficient Full-Color Colloidal Quantum Dot Light-Emitting Diodes Using an Inverted Device Structure. *Nano Lett.* **2012**, *12*, 2362–2366.
- Lee, K.-H.; Lee, J.-H.; Kang, H.-D.; Park, B.; Kwon, Y.; Ko, H.; Lee, C.; Lee, J.; Yang, H. Over 40 cd/A Efficient Green Quantum Dot Electroluminescent Device Comprising Uniquely Large-Sized Quantum Dots. *ACS Nano* **2014**, *8*, 4893–4901.
- Yang, X.; Zhao, D.; Leck, K. S.; Tan, S. T.; Tang, Y. X.; Zhao, J.; Demir, H. V.; Sun, X. W. Full Visible Range Covering InP/ZnS Nanocrystals with High Photometric Performance and Their Application to White Quantum Dot Light-Emitting Diodes. *Adv. Mater.* **2012**, *24*, 4180–4185.
- Anikeeva, P. O.; Halpert, J. E.; Bawendi, M. G.; Bulović, V. Quantum Dot Light-Emitting Devices with Electroluminescence Tunable over the Entire Visible Spectrum. *Nano Lett.* **2009**, *9*, 2532–2536.
- Qian, L.; Zheng, Y.; Xue, J.; Holloway, P. H. Stable and Efficient Quantum-Dot Light-Emitting Diodes Based on Solution-Processed Multilayer Structures. *Nat. Photonics* **2011**, *5*, 543–548.
- Zhang, Y.; Xie, C.; Su, H.; Liu, J.; Pickering, S.; Wang, Y.; Yu, W. W.; Wang, J.; Wang, Y.; Hahm, J.; *et al.* Employing Heavy Metal-Free Colloidal Quantum Dots in Solution-Processed White Light-Emitting Diodes. *Nano Lett.* **2011**, *11*, 329–332.
- Schreuder, M. A.; Xiao, K.; Ivanov, I. N.; Weiss, S. M.; Rosenthal, S. J. White Light-Emitting Diodes Based on Ultrasmall CdSe Nanocrystal Electroluminescence. *Nano Lett.* **2010**, *10*, 573–576.
- Tan, Z.; Zhang, Y.; Xie, C.; Su, H.; Liu, J.; Zhang, C.; Dellas, N.; Mohny, S. E.; Wang, Y.; Wang, J.; *et al.* Near-Band-Edge Electroluminescence from Heavy-Metal-Free Colloidal Quantum Dots. *Adv. Mater.* **2011**, *23*, 3553–3558.
- Zhang, X.; Zhang, Y.; Wang, Y.; Kalytchuk, S.; Kershaw, S. V.; Wang, Y.; Wang, P.; Zhang, T.; Zhao, Y.; Zhang, H.; *et al.* Color-Switchable Electroluminescence of Carbon Dot Light-Emitting Diodes. *ACS Nano* **2013**, *7*, 11234–11241.
- Colvin, V. L.; Schlamp, M. C.; Alivisatos, A. P. Light-Emitting Diodes Made from Cadmium Selenide Nanocrystals and a Semiconducting Polymer. *Nature* **1994**, *370*, 354–357.
- Shirasaki, Y.; Supran, G. J.; Bawendi, M. G.; Bulović, V. Emergence of Colloidal Quantum-Dot Light-Emitting Technologies. *Nat. Photonics* **2013**, *7*, 13–23.
- Talapin, D. V.; Lee, J. S.; Kovalenko, M. V.; Shevchenko, E. V. Prospects of Colloidal Nanocrystals for Electronic and Optoelectronic Applications. *Chem. Rev.* **2010**, *110*, 389–458.

17. Han, T.-H.; Lee, Y.; Choi, M.-R.; Woo, S.-H.; Bae, S.-H.; Hong, B. H.; Ahn, J.-H.; Lee, T.-W. Extremely Efficient Flexible Organic Light-Emitting Diodes with Modified Graphene Anode. *Nat. Photonics* **2012**, *6*, 105–110.
18. Wang, Z. B.; Helander, M. G.; Qiu, J.; Puzzo, D. P.; Greiner, M. T.; Hudson, Z. M.; Wang, S.; Liu, Z. W.; Lu, Z. H. Unlocking the Full Potential of Organic Light-Emitting Diodes on Flexible Plastic. *Nat. Photonics* **2011**, *5*, 753–757.
19. Kim, T. H.; Cho, K. S.; Lee, E. K.; Lee, S. J.; Chae, J.; Kim, J. W.; Kim, D. H.; Kwon, J.-Y.; Amaratunga, G.; Lee, S. Y.; *et al.* Full-Colour Quantum Dot Displays Fabricated by Transfer Printing. *Nat. Photonics* **2011**, *5*, 176–182.
20. Tan, Z.; Xu, J.; Zhang, C.; Zhu, T.; Zhang, F.; Hedrick, B.; Pickering, S.; Wu, J.; Su, H.; Gao, S.; *et al.* Colloidal Nanocrystal-Based Light-Emitting Diodes Fabricated on Plastic Toward Flexible Quantum Dot Optoelectronics. *J. Appl. Phys.* **2009**, *105*, 034312.
21. Leck, K. S.; Divayana, Y.; Zhao, D.; Yang, X.; Abiyasa, A. P.; Mutlugun, E.; Gao, Y.; Liu, S.; Tan, S. T.; Sun, X. W.; *et al.* Quantum Dot Light-Emitting Diode with Quantum Dots Inside the Hole Transporting Layers. *ACS Appl. Mater. Interfaces* **2013**, *5*, 6535–6540.
22. Yang, X.; Mutlugun, E.; Zhao, Y.; Gao, Y.; Leck, K. S.; Ma, Y.; Ke, L.; Tan, S. T.; Demir, H. V.; Sun, X. W. Solution Processed Tungsten Oxide Interfacial Layer for Efficient Hole-Injection in Quantum Dot Light-Emitting Diodes. *Small* **2014**, *10*, 247–252.
23. Hofmann, S.; Thomschke, M.; Lüssem, B.; Leo, K. Top-Emitting Organic Light-Emitting Diodes. *Opt. Express* **2011**, *19*, 1250–1264.
24. Thomschke, M.; Reineke, S.; Lüssem, B.; Leo, K. Highly Efficient White Top-Emitting Organic Light-Emitting Diodes Comprising Laminated Microlens Films. *Nano Lett.* **2012**, *12*, 424–428.
25. Huang, Q.; Walzer, K.; Pfeiffer, M.; Lyssenko, V.; He, G.; Leo, K. Highly Efficient Top Emitting Organic Light-Emitting Diodes with Organic Outcoupling Enhancement Layers. *Appl. Phys. Lett.* **2006**, *88*, 113515.
26. Ma, H.; Yip, H.-L.; Huang, F.; Jen, A. K.-Y. Interface Engineering for Organic Electronics. *Adv. Funct. Mater.* **2010**, *20*, 1371–1388.
27. Meyer, J.; Khalandovsky, R.; Görrn, P.; Kahn, A. MoO<sub>3</sub> Films Spin-Coated from a Nanoparticle Suspension for Efficient Hole-Injection in Organic Electronics. *Adv. Mater.* **2011**, *23*, 70–73.
28. Murase, S.; Yang, Y. Solution Processed MoO<sub>3</sub> Interfacial Layer for Organic Photovoltaics Prepared by a Facile Synthesis Method. *Adv. Mater.* **2012**, *24*, 2459–2462.
29. Kröger, M.; Hamwi, S.; Meyer, J.; Riedl, T.; Kowalsky, W.; Kahn, A. Role of the Deep-Lying Electronic States of MoO<sub>3</sub> in the Enhancement of Hole-Injection in Organic Thin Films. *Appl. Phys. Lett.* **2009**, *95*, 123301.
30. Haranath, D.; Sahai, S.; Joshi, P. Tuning of Emission Colors in Zinc Oxide Quantum Dots. *Appl. Phys. Lett.* **2008**, *92*, 233113.
31. Lin, B.; Fu, Z.; Jia, Y.; Liao, G. Defect Photoluminescence of Undoping ZnO Films and Its Dependence on Annealing Conditions. *J. Electrochem. Soc.* **2001**, *148*, 110–113.
32. McCluskey, M. D.; Jokela, S. J. Defects in ZnO. *J. Appl. Phys.* **2009**, *106*, 071101.
33. Djurišić, A. B.; Choy, W. C. H.; Roy, V. A. L.; Leung, Y. H.; Kwong, C. Y.; Cheah, K. W.; Rao, T. K. G.; Chan, W. K.; Lui, H. F.; Surya, C. Photoluminescence and Electron Paramagnetic Resonance of ZnO Tetrapod Structures. *Adv. Funct. Mater.* **2004**, *14*, 856–864.
34. Liu, C.-C.; Liu, S.-H.; Tien, K.-C.; Hsu, M.-H.; Chang, H.-W.; Chang, C.-K.; Yang, C.-J.; Wu, C.-C. Microcavity Top-Emitting Organic Light-Emitting Devices Integrated with Diffusers for Simultaneous Enhancement of Efficiencies and Viewing Characteristics. *Appl. Phys. Lett.* **2009**, *94*, 103302.
35. Lee, J.; Hofmann, S.; Furno, M.; Thomschke, M.; Kim, Y. H.; Lüssem, B.; Leo, K. Influence of Organic Capping Layers on the Performance of Transparent Organic Light-Emitting Diodes. *Opt. Lett.* **2011**, *36*, 1443–145.